Hindawi
Journal of Engineering
Volume 2023, Article ID 4964194, 14 pages
https://doi.org/10.1155/2023/4964194

Research Article

Color Adsorption Performance of Bone Biocomponent for Textile Dyeing Effluent Treatment in Ethiopia

Natinael Kokeb,[1,2] **Tamrat Tesfaye**,[1] **Shalemu Sharew**,[1] **Gemeda Gebino**,[1] **and Tinsaye Asfaw**[1]

[1]*Ethiopian Institute of Textile and Fashion Technology, Bahir Dar University, Bahir Dar, Ethiopia*
[2]*Department of Chemistry and Engineering of Materials, Wroclaw University of Science and Technology, Wroclaw, Poland*

Correspondence should be addressed to Gemeda Gebino; gemedalvgebino@gmail.com

Received 30 January 2023; Revised 20 March 2023; Accepted 16 June 2023; Published 30 June 2023

Academic Editor: Michela Dalle Mura

The continued expansion of industrial growth has contributed significantly to the economic development of many countries. However, untreated discharge from the textile factory significant impacts freshwater and public health. The aim of this study is to explore the economical-local wastewater treatment for local textile industries. The experiment used the waste bones as a source of calcium-phosphate nanopowder (CNP) biocomponent, adsorbent for azo dye effluent treatment. An isolated biocomponent was analyzed using FTIR and UV-VIS, and its adsorption isotherm was also calculated. The FTIR analysis of CNP showed carbonates, amide, and high-intensity phosphate peaks of 1008 cm^{-1} and 1337 cm^{-1}. The effect of contact time analyzed by UV-VIS absorption spectra revealed that 70% of color removal was achieved within 30 minutes and 60 minutes for disperse red 1 dye (DR1D) and DCT reactive blue 109 dyes (RB109D), respectively. In addition, the effects of the condition parameters on percentage color removal were analyzed using DOE response surface methodology. The maximum color removal performances are 98.65% and 96%, respectively, for DR1D and RB109D at neutral pH. The Langmuir isotherm was observed in the adsorption of RB109D effluent with an R2 value of 0.994 and the Freundlich isotherm in the adsorption of DR1D with an R2 value of 0.993. Finally, the gauge of the effectiveness of treatment was analyzed by COD, BOD, and TSS values before and after treatment. The maximum deduction percentages of COD, BOD, and TSS were 82, 87, and 70% from RB109D; 89, 90, and 89% from DR1D; and 82, 89, and 71% from the industry sample, respectively. Generally, the study showed that the current adsorbent was a good substitute for synthetic adsorbents.

1. Introduction

The recent textile coloration practices had been using 700 kilotons of synthetic dyes per year worldwide. Worldwide, about 200 kilotons of dyes are lost to effluents every year [1–3]. Azo dyes are the largest category of synthetic colorants and the most often discharged synthetic dye into the environment, accounting for over 70% of all dyestuffs used globally. An Ethiopian textile industry statistic shows the country imports over 700 tons of dyestuffs [4], of which about 70% from total amount are azo dyes. Azo dyes contain about 10–100 mg/L of hazardous compounds such as oncogenic amines [5] and other chemical pollutants in the form of toxic metals, pentachlorophenol, biocides, and chlorine. It also has toxic effects on aquatic flora and fauna, resulting in severe environmental issues across the globe. Additionally, azo dyes have negative effects on biological oxygen demand (BOD), chemical oxygen demand (COD), and total suspension solids (TSS) [6–8]. Most of the dyes are released into the environment without effective wastewater treatment [9]. The reason may be due to noneconomical wastewater treatment for developing countries such as Ethiopia [10–12].

The physicochemical and biological treatment approaches have been developed to lower the extent of coloring and organic materials from effluents [13, 14]. The

physicochemical methods such as photocatalysis [15], flocculation/coagulation [16–18], sonication, sludge adsorption [19], ion exchange [20, 21], activated carbon adsorption [22–24], ozonation [25, 26], irradiation, and electrochemical oxidation [27, 28] were well studied for small scale industries. The biological approaches [29–32] of treatment using fungi [33], algae, yeast, bacteria, plants [34–36], and animal [37] wastes were considered as cost-effective, sustainable, and environmentally beneficial approach [38–40] while being specific in use. Among animal wastes, bovine bones were abundantly available wastes which creates nonhealthy environment [41] and also increases with the increase of meat consumption [42]. Among these products, livestock bones account for a large proportion [43]. The composition of bone [44, 45] is rich in calcinates and phosphates; building components of [46, 47]. The hydroxyapatites from bones of different animals were experimented by others for color adsorption from acid [48, 49], reactive [50–52], and indigo [53] dye effluents.

The recent novel approaches to textile wastewater treatment, such as nonthermal plasma treatment [54–57], hydrogel adsorbents [58–60], and modified photocatalysis [61–64], were also getting the attention of the sector. However, they were specific to either coloring materials or organic molecules, cost ineffectiveness while using a combined approach, complexity for large-scale application [65], working for a specific dye group, and producing secondary pollution [66, 67].

As far as we know, there are limited works on absorbers able to simultaneously remove the color and other contaminants from dye types used for the current experiment. The biocomponent from the bone is proposed for reducing coloring material and organic ions in industrial wastewater. Therefore, this study aims to analyze the likelihood of using an animal bone biocomponent, CNP, as an effective adsorbent of color and organic molecules from the DR1D and RB109D effluents. Until now, there has been no work on such DR1D and RB109D effluent discoloration using calcium sources.

2. Experimental

2.1. Materials. The fresh raw bovine bones were collected from a local restaurant (Bahir Dar, Ethiopia), whereas the dried bones of bovine were found in a local home (Figure 1). Other materials were from wet processing laboratories at the Ethiopian Institute of Textile and Fashion Technology (EiTEX), Bahir Dar University.

The chemicals used were HCl, DCT reactive blue 109 dyes (MX RB109D, λmax = 610 nm, MW = 1040.60 g/mol, anionic, and soluble in water), disperse red 1 dye (DR1D, λmax = 490 nm, MW = 314.34 g/mol, nonionic in nature, and partially soluble in water), sodium benzoate, ammonium nitrate, NaCl, $CaCl_2$, potassium phosphate dibasic trihydrate, calcium chloride dehydrate, sodium acetate, magnesium chloride hexahydrate, and distilled water (Table 1). All the chemicals used were made to a laboratory standard, which was obtained from the EiTEX laboratory. Industry effluent was collected from Bahir Dar Textile Share Company (BTSC).

2.2. Extraction and Preservation of Calcium-Phosphate Nanopowder. The recipes for extracting of biocomponents were already studied [68, 69]. The fresh bone was treated with distilled water at 60°C to detach the meat from the bone surface and crushed into small pieces as shown in Figure 1. Then, 50 gm of crushed bone was boiled to 100°C with 1 M HCl (8.3 ml HCL added into 100 ml distilled water). The bone was dissolved and then the acidic biocomponent solution was filtered using a micromesh filter. The filtered acidic solution was treated with various concentrations of NH_3 (ammonia) to form a precipitate of the biocomponent. The precipitates were collected in a petridish and placed in an oven dryer at a temperature of 100°C for the duration of 10 minutes to evaporate the water. After cooling, the dried biocomponent was ground to form CNP.

2.3. Experimental Design. The experimental design has been made using the state-ease scientific tool (Stat-Ease Design Expert 11.1.2.0). The details for the experimental design of extraction were shown in Table 2. The design for the percentage discoloration potential of the CNP against DR1D and RB109D effluents was made with two repeats, 12 runs were used for each experiment as shown in Tables 3 and 4.

2.4. Yield of Precipitate. The yield [70] of CNP was analyzed as per the following equation:

$$\text{yield of CaNP} = \frac{\mathbf{Bi} - \mathbf{Bf}}{\mathbf{Bi}} \text{x}100\%, \quad (1)$$

where Bi and Bf are initial and final weight of bone, respectively.

2.5. Response Optimization. The response surface methodology (RSM) was used to determine the best independent variable values in order to maximize the response [71]. The models used were quadratic and two-factor interaction (2FI) in the case of RB109D and DR1D parameters, respectively. The precipitate optimization goals were maximizing the extract and precipitate whereas the pH was kept in range. It also allows the user to look at how the individual variables interact, making it more effective than the more common single-parameter optimization method. These factors have led to the use of RSM in the extraction of biocomponents and percentage color removal in the current case.

2.6. Fourier-Transform Infrared Spectroscopy Analysis (FTIR). The composition of the biocomponent was analyzed by a Fourier transform infrared spectrophotometer (Perkin Elmer, UATR TWO, Ethiopia), calibrated according to the manufacturer's instructions in the Ethiopian institute of textile and fashion technology (EITEX) lab. After pressing the samples into pellets, the absorption spectra were examined within the wave range from 500 cm^{-1} to 3500 cm^{-1}.

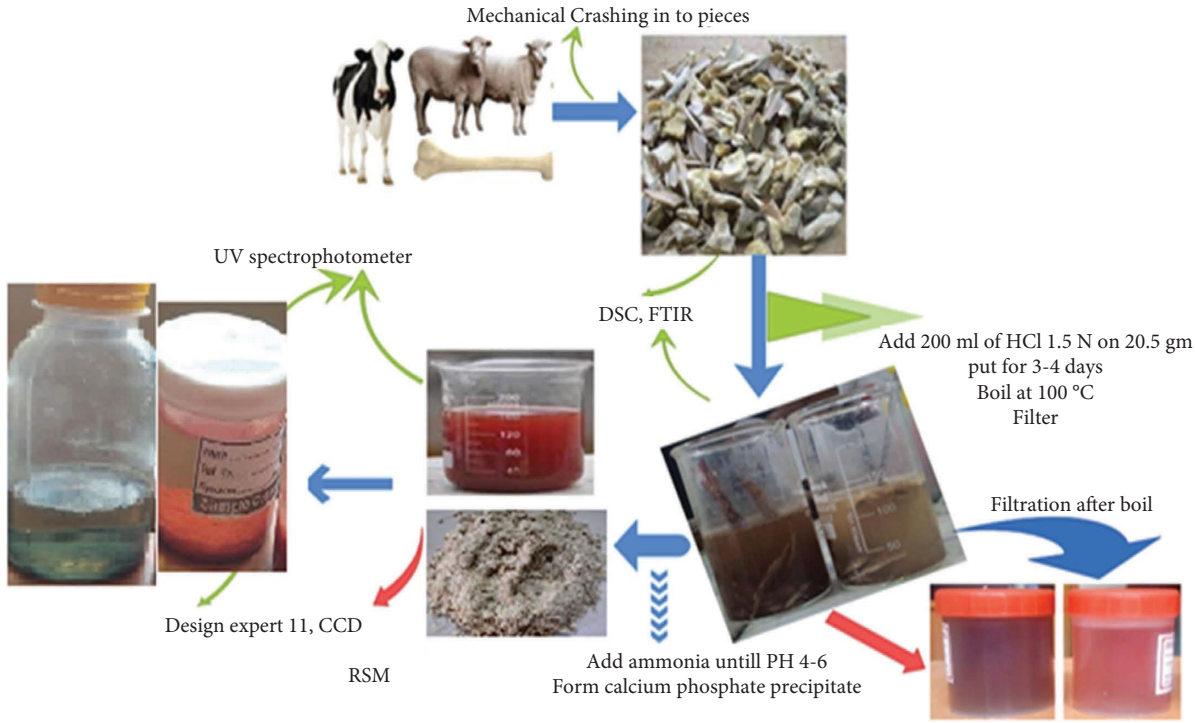

Figure 1: The pictorial representation of bone biocomponent extraction and its characterization process.

Table 1: Characteristics of the dyes.

Parameters	DCT reactive blue 109	Disperse red 1
Molecular formula	$C_{25}H_{12}Cl_2N_9Na_5O_{16}S_5$	$C_{16}H_{18}N_4O_3$
Molecular weight	1040.60 g/mol	314.34 g/mol
Brand	Sigma-Aldrich	Sigma-Aldrich
Molecular structure	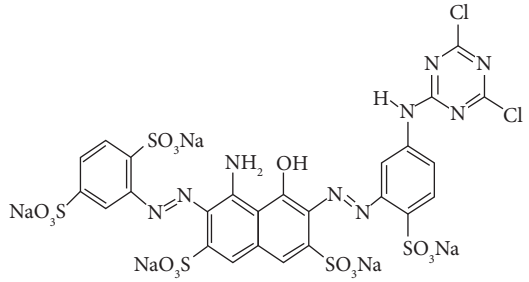	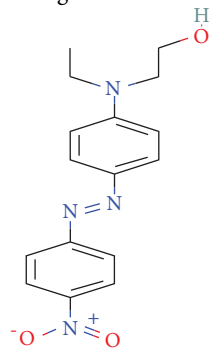

Table 2: Experimental design of AB yield.

Run	Factor 1 A: extract (ml)	Factor 2 B: pH (pH)	Response 1 Weight of AB (gm)
1	11	5	7.12
2	10	7	15
3	12	3	7
4	10	3	6.77
5	12	7	16.74
6	11	7.82843	16.32
7	12.4142	5	15.33
8	11	2.17157	4
9	9.58579	5	6.89

2.7. Dye Effluent Sampling. The dye effluent samples were prepared by mixing synthetic wastewater with dye solutions. The synthetic wastewater was prepared as per the recipe mentioned by [72] with some modifications. The dye solutions were prepared using DR1D and RB109D in distilled water with a concentration of 50 mg/l for each dye solution (Figure 2). Industrial wastewater was taken from BTSC for comparison with TS after treatment.

2.8. UV Spectrophotometer and Removal Percentage. The absorption of the sample was analyzed by a UV-Vis spectrophotometer (Perkin Elmer, Model Lambda 25, Ethiopia).

Table 3: Percentage removal of RB109D effluent in 5 ml waste water.

Run	Factor 1 a: RB109D (ml)	Factor 2 b: extract (ml)	Response 1 % Removal
1	25	10	94.56
2	10	10	95.38
3	6.8934	7.5	96.22
4	28.1066	7.5	98.88
5	17.5	7.5	89.21
6	17.5	3.96447	98.88
7	17.5	3.96447	98.86
8	17.5	11.0355	84.66
9	17.5	11.0355	84.66
10	17.5	7.5	83.91
11	25	5	89.69
12	10	5	97.27

The spectra were examined within the wave range from 400 cm^{-1} to 900 cm^{-1}. The results were used for analysis to determine the adsorption isotherms and effects of treatment duration, as well. The percentage removal [56, 73] was calculated by equation (2), where the percentage values were from UV spectrophotometers [35].

$$\text{Color removel}\,(\%) = \frac{\text{Abs0} - \text{Abs}}{\text{Abs0}} \times 100\%, \tag{2}$$

where Abs_0 represents absorbance value before adsorption and Abs represents absorbance value after adsorption.

2.9. Equilibrium Adsorption Isotherm. The studies were carried out to investigate the adsorption effectiveness of both the effluents. Between 0.5 and 5 grams of the adsorbent were used in the studies and they were placed in 100 mL of the dyes (variable concentration) aqueous solution in conical flasks that were 250 mL in size and were parafilm-sealed. A UV-VIS spectrophotometer was used to measure the solution's residual dye concentration after 60 minutes at 610 nm for RB109D and 490 nm for DR1D, respectively. At a pH of 7, each experiment was carried out three times. The removal of the dye can be used to explain the adsorption of the dye [74].

2.10. BOD, COD, and TSs Analysis. The experiments on biological oxygen demand (COD), biological oxygen demand (BOD), and total solids (TSs) were conducted in the laboratory of the Bahir Dar Textile Share Company (BTSC). Three categories of samples: RB109D, DR1D, and BTSC samples were used at this stage. The third sample was taken directly from the BTSC industry waste tank to compare with samples from the experiment. The BOD test was made to determine the amount of oxygen bacteria consumed in a particular volume of water over a given time. Since the treated water is intended for the environment, its organic matter content should be analyzed. A liter of wastewater was used. All the samples were combined for 30 to 45 minutes and stored in dark for five days. The BOD measurement was conducted at a temperature of 20°C.

The COD treatment medium was examined using a Lovibond thermos-reactor (Thermoreactor RD 125, EiTEX, Ethiopia). A 12 liter more of wastewater was added to the installation. The samples were stored inside the reactor for two weeks at a temperature of 25°C with constant aeration. At the start and end of the experiment, COD values were measured, and the outcome was presented as a percentage reduction of molecules. The COD analysis was performed in accordance with SR ISO 6060.

3. Results and Discussion

3.1. Biocomponent Extraction and Characterization

3.1.1. Bone Biocomponent Extraction. The result has been calculated, and the average yield of precipitate was 10.57444 g, which is 92.68167 percent. The dissolved biocomponent was generated by treating waste bone with dilute HCl (0.5 M) as shown in Figures 3(a) and 2(b). The contribution of HCl acid during extraction is in order to breakdown the complicated component of bone hydroxyapatite into mineral ions in the bone, such as calcium ions and hydrophosphate ions. The possible reaction that takes place is shown in equations (3)–(6).

$$Ca_{10}(PO_4)_6(OH)_2 + 2HCl = CaCl_2 + 3Ca_3(PO_4)_2(H_2O)^+ \text{ (aqueous)} \tag{3}$$

$$3Ca_3(PO_4)_2(H_2O)^+ = 2Ca_4(PO_4)_3 + Ca^{2+} + 2H_2O \tag{4}$$

$$2Ca_4(PO_4)_3 + 2H^+ = 2Ca^{2+} + 3Ca_2H(PO_4)_3 \tag{5}$$

$$3Ca_2HPO_4 + H^+ = 3Ca_2^{2+} + 3HPO_4 \tag{6}$$

The addition of ammonium to the solution causes the agglomeration of the mineral ions (equation (7)) in the form of a precipitate, as shown in Figures 3(c) and 3(d). A random ammonium addition results in large precipitate agglomerates of calcium phosphate, whereas a slow addition results in fine precipitates. Exposing the precipitate in an oven at 100°C for 10 minutes causes simple dehydration of the water molecules, which occurs either when two hydrogen atoms from one molecule join with an oxygen atom on the other molecule or when a hydroxyl group from one molecule

Table 4: Percentage removal of DR1D effluent at 5 ml waste water.

Run	Factor 1 A: DR1D (ml)	Factor 2 b: extract (ml)	Response 1 % Removal
1	6.8934	7.5	97.43
2	28.1066	7.5	95.55
3	17.5	7.5	85.4
4	17.5	11.0355	98.28
5	17.5	11.0355	98.3
6	17.5	3.96447	98.66
7	17.5	3.96447	97.01
8	17.5	7.5	86.11
9	10	5	97.81
10	25	5	97.51
11	25	10	97.54
12	10	10	98.42

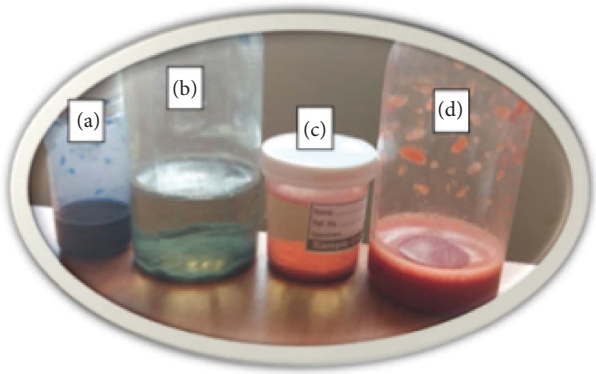

Figure 2: The dye effluents (a and d) and adsorbed solutions (b and c) of reactive and disperse dyes, respectively.

reacts with a hydrogen atom from the other molecule. Next, collect the powder from the Petri dish and crush it into a nanosize powder. The matured mineral matrix is present in a nanosized form as CNP, which is hydroxyapatite ($Ca_{10}(PO_4)_6(OH)_2$) as a reaction potential [75–77].

3.1.2. Effect of Biocomponent Solution on Yield. At constant pH, increasing the concentration of the biocomponent solution (extract) caused a slight increase in the mass of the biocomponent precipitate (Figure 4). The reason might be that the more the extract, the more $H_2PO_4^-$ molecules there are, which could dissociate until the electrolyte saturates. Furthermore, increasing the solution may not have a significant effect.

3.1.3. Effect of Ammonia on Yield of the CNP. As shown in Figure 4, there is a significant increase in the mass of the CNP biocomponent precipitate when the pH rises due to the addition of ammonia. The pH of the acidic biocomponent solution was slowly increased as ammonia was slowly added, and then the amount of precipitate that formed also increased. Later, when all of the hydrochloric acids had been neutralized by ammonia, the pH reached seven, after which the pH would increase further as the solution became alkaline, the pH of which would depend on the concentration of ammonia in the solution. However, for our case, we were focused on neutral pH, which is ecofriendly to release the water into the environment after treatment.

The formation of the precipitate is caused by the dissociation of the ionic molecule H_2PO_4 by ammonia, as shown in equation (7). The chemistry is that the tendency of H_2PO_4 to dissociate is greater than its tendency to hydrolyze, so that the $(NH_4)_2(HPO_4)$ exists in crystal form since it is insoluble in water at room temperature. On the other hand, ammonium dihydrogen phosphate can stay dissolved in water [77, 78].

$$Ca^{2+} + H_2PO_4^- + NH_3 = Ca\left(HP\,O_4\right) + (NH)_2\left(HPO_4\right) \tag{7}$$

3.1.4. Optimum CNP. The conditions delivering the maximum precipitate of the biocomponent (CaNP) were determined (Figure 5). The ideal extraction parameters were 10 ml of the extract with a pH of 6.9. The mass of the total precipitate yield was estimated to be 13.2664 g under optimal circumstances, which is very similar to the actual value of 13.5 g discovered under the modified conditions (Table 5) with 89.9% desirability. These outcomes demonstrate the model can forecast the experimental conditions.

The neutral pH is recommended because it allows the treated water to be released into the environment with the least pollution. Technically, it is economical to remove a large volume of color from the effluent using a low-mass CNP.

3.1.5. The Analysis of FTIR. The FTIR spectrum of CNP extracted from the animal bone heated at 100 is shown in Figure 6. The main indication of CNP can be identified by the characteristic peaks of the phosphate band within two spectral regions: from 844 cm^{-1} up to 1038 cm^{-1} and 1320 cm^{-1} to 1500 cm^{-1}. All spectral bands of phosphate, especially the two high-intensity phosphate peaks at 1008 cm^{-1} and 1337 cm^{-1} demonstrate the isolated CNP adsorbent has a higher phosphate concentration. They also represent the presence of tricalcium phosphate. The spectra also identified the carbonate bands at 1106 cm^{-1}, 1566 cm^{-1}, and 1638 cm^{-1}, and low intensity of organic carbon vibrations were observed within the region from 1833 cm^{-1} to 2106 cm^{-1}. In between bands of 2851 cm^{-1} and 2918 cm^{-1}, amide ion stretching was also observed [79–81]. Therefore, phosphates, carbonates, and amide ions were incorporated into the CNP.

4. Color Removal Analysis

4.1. Effect of RB109D Effluent Concentration on Percentage Color Removal. The value of the coefficient of determination (R2) was 0.9895. Such values indicated the 98.95% of variability could be explained by the selected model in case. Moreover, the adjusted R2 value of 0.9711, 0.6808 denotes the validity of the linear model applied in this case.

(a) (b) (c) (d)

Figure 3: Dry bone in HCl (a), biocomponent in solution form from fresh bone (b), and biocomponent in powdered form from fresh and prestored dry bone (c, d), respectively.

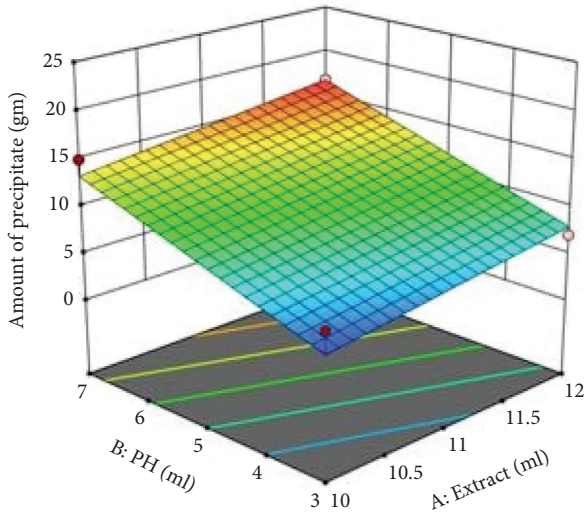

Figure 4: The effect of extract solution and its pH on precipitate amount.

As shown in Figure 7 and Table 3, an increase of the RB109D effluent concentration from 10 ml to 25 ml caused a lowering of color removal percentage from 97% to 92.5%. The extract also shows a similar effect, decreasing the percentage of color removal as its concentration increases. Therefore, the addition of more extract into the solution cannot improve the efficiency of treatment, which contradicts the effect analyzed by other adsorbents [82]. The possible reason for such an effect might be due to the inundation of calcium phosphate. The inundation indicates that there were no unoccupied binding sites available (all active sites of the extract linked with bonds from the dye) for the adsorption of the dye molecules [83].

The adsorption might happen for two reasons. The first reason is due to the surface calcium chelating with bidentate from functional groups -NH- and C=O, --OH and C=O, -N- and -OH. Calcination was taken place at the boiling temperature of the water, which allowed to get calcium ions within the adsorbent. Previous studies showed no calcium after calcinating a raw bone at a temperature of 1000°C. Whereas, Figure 8 depicts the link between azo-nitrogen and hydroxyl groups in hydroxyapatite and -NH- or ionized carbonyl oxygen in the dye molecule [84].

4.2. Effect of DR1D Effluent Concentration on Percentage Color Removal. The value of the coefficient of determination (R2) was 0.8259. Such values indicated about 82.59% of variability and could be explained by the selected models. Moreover, the adjusted R2 value of 0.6808 denoted the validity of the quadratic model.

The interaction effects of DR1D effluent concentration and the extract were investigated for a duration of 90 min in the response plot and contour lines (Figure 9 and Table 4). A communal rise in the ratio of dye effluent concentration and extract from 9.2 : 5 (ml) to 17.5 : 7.5 (ml), respectively, caused a decline in the efficiency of the percentage color removal from 95.5% to 85%. Then, the decolorization efficiency ascends again from 85% to 98% when the ratio continues to rise until 25.5 : 10 (ml). The reason for such an effect can be a higher concentration of dye effluent as compared to extract; it may cause the saturation of the accessible binding sites on the surface of calcium phosphate [82, 85].

Saturation is enhanced as per the slowing of diffusion. It is known that the diffusion mechanism of DR1D particles into the adsorbent has two steps [86]. The first is the dye transfer from the solution to the adsorbent. The dye diffusion from the adsorbent's surface to the pore is the latter. Due to the very low adsorbate concentration in the solution, intraparticle diffusion reduces in the final equilibrium stage.

4.3. Effect of Extracted Adsorbent on Percentage Color Removal. As illustrated in Figure 7, the percentage of color removal decreased as we kept increasing the concentration of extracted adsorbent to 10 ml in the case of RB19D effluent treatment. Whereas, in the case of DR1D effluent treatment, the percentage color removal showed a parabolic effect as indicated in Figure 9. It was demonstrated that the azo group is disrupted and a diazo compound and a quinone are formed when azo dyes are oxidized in aqueous media with a calcium phosphate reagent. These, then, continue to break down, yielding phenol and nitrogen, respectively (in acidic media). The pH of the adsorbent was mandatory for

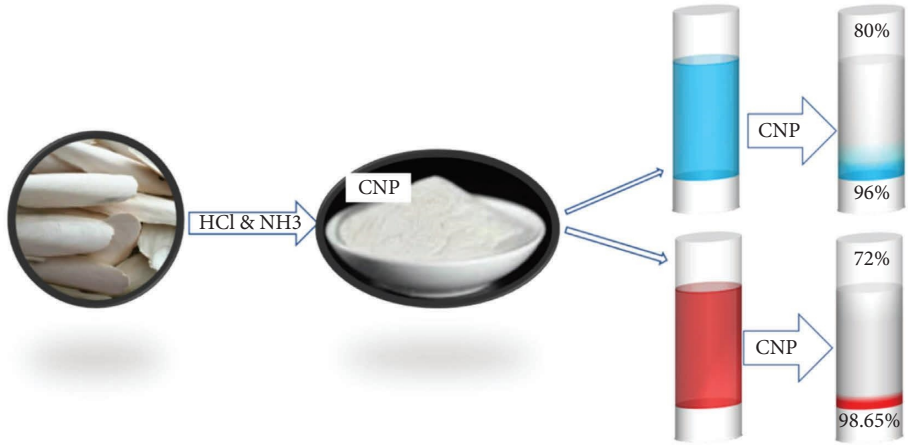

Figure 5: Graphical description of CaNP (calcium nanopowder).

Table 5: Optimum condition parameters of biocomponent precipitate.

Condition	pH	Extract (ml)	Precipitate (gm)
Optimum	6.9	10	13.2664 (predicted)
Modified	7	10	13.5 (actual)

decolorization by biosorption because it attracts charged dyes to the surface of the adsorbent. An increase in the concentration of H^+ ions (acidic) attracts anionic colors to the adsorbent surface via electrostatic attraction, whereas an increase in the concentration of OH^+ ions (basic) attracts the dye ions to the biomass surface via electrostatic attraction [87]. Because the concentration of H^+ ions in the solution might affect both adsorbed molecules and adsorbent particle functional groups, they participate in the molecular adsorption process at the adsorbent's active sites.

At basic pH, the repellent electrostatic interactions between the adsorbent negatively charged surface and the anionic dye abundant prevent the quantity of adsorbed dye molecules from reducing. The ionization of the dye's amine and amide groups with H^+, which renders the dye molecules positively charged, can reduce adsorption below pH of three. As a result, adsorption was decreased [88].

4.4. Effect of the Contact Time on Color Removal. The effect of adsorbent contact time on color removal was analyzed using the UV-Vis spectrum as shown in Figures 10 and 11. It was observed that all samples of RB109D effluent showned a typical peak in their UV-Vis spectrum at its absorption wavelength of 610 nm. More than 75% of the effluent color reduction has been achieved after one-hour treatment (Figure 10). Then, the percentage of color removal gradually increased, and the maximum potential of the adsorbent to remove the color is achieved at 140 min. The maximum color removal of 96% was achieved for RB109D. The discoloration was caused due to the breakdown of the azo linkage (color-bearing group) after the dye adsorbed on the surface of the adsorbent. The degradation chemistry occurs in two phases at the azo (N=N) linkage. First, two electrons are transferred to the azo dye, which acts as a final electron acceptor, resulting in dye decolorization and the formation of colorless solutions at each stage. Then, intermediate metabolites (such as benzene amines) are then eliminated either aerobically or anaerobically [39].

Whereas, the DR1D effluent had no significant peak in its UV-Vis spectrum at its absorption wavelength of 490 nm (Figure 11). It was demonstrated that the extension of treatment time after the first 20 minutes has less effect on adsorption. More than 75% of the effluent's color reduction was achieved at 20 minutes of treatment time, as shown in Figure 10. After the first 20 minutes, there was a very slow increase in the percentage of color removal, and the maximum potential of the adsorbent to remove the color was achieved at 140 minutes. The maximum color removal of 98.65% was achieved for DR1D. The dye had a faster diffusion rate than RB109D to the adsorbate surface. As a result, the equilibrium period for dye adsorption on the CNP biocomponent was 140 min.

The rate of the dye adsorption was quicker in the early stages because of the huge concentration differential between the dye and the adsorbent active sites. The delayed diffusion of the dye into the bulk of the adsorbent is likely to blame for the slower adsorption rate in the latter stages of dye adsorption [89].

4.5. Adsorption Isotherm Models. Adsorption isotherms were illustrated for the dye adsorbed by the unit mass of the adsorbent at room temperature and the concentration of the dye in the solution at a nearly neutral pH [90, 91]. The Langmuir and Freundlich isotherms are the most utilized equations for dilutions that indicate a connection between the equilibrium values. The Langmuir isotherm was expressed as follows [92]:

$$\frac{\mathbf{Ce}}{\mathbf{Ae}} = \frac{\mathbf{Ce}}{\mathbf{Am}} + \frac{\mathbf{1}}{\mathbf{KAm}}, \tag{8}$$

where K = Langmuir equilibrium constant, Ce = aqueous concentration, Ae = amount adsorbed, and Am = the maximum adsorption capacity of the adsorbent.

The Freundlich equation was written as follows [92]:

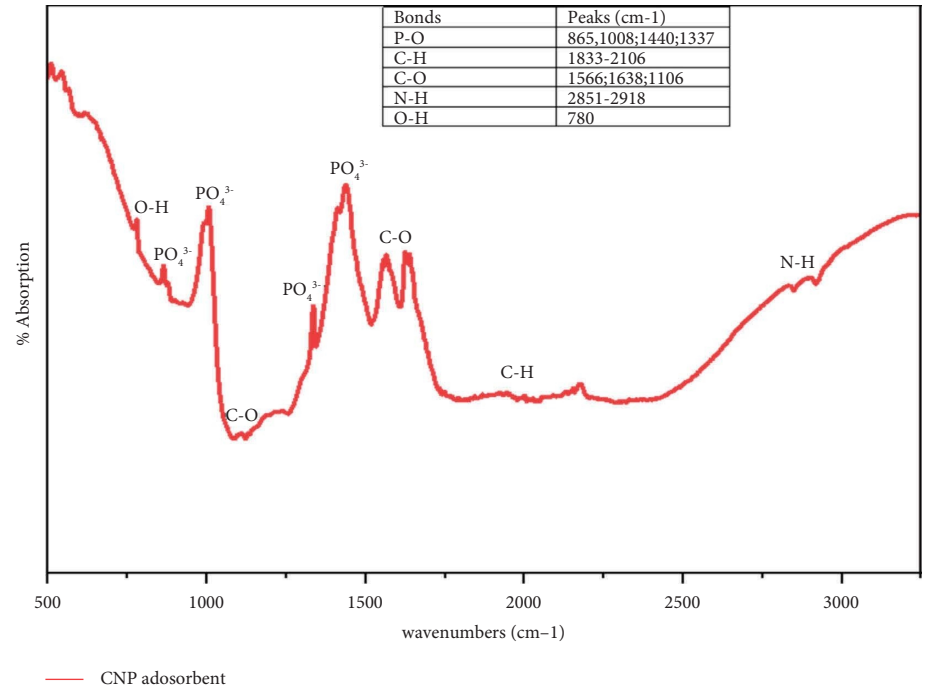

Figure 6: FT-IR spectral graph of the CNP adsorbent crystal.

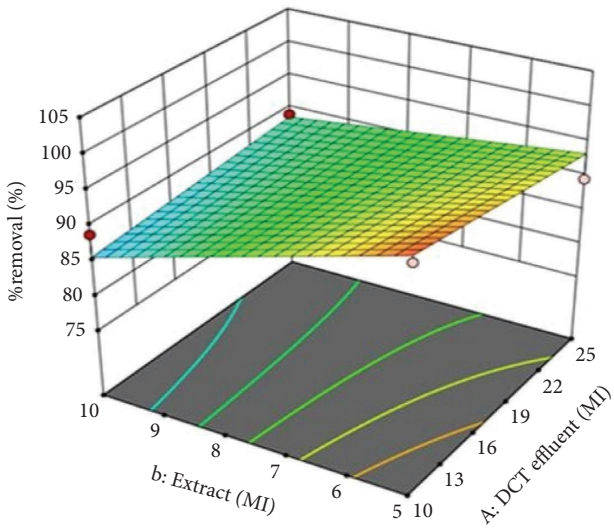

Figure 7: Interaction effect of the extract and the RB19D effluent concentrations on % removal of the color.

$$\log(\mathrm{Ae}) = \log\mathrm{Kf} + \frac{1}{n}\log\log(\mathrm{Ce}), \tag{9}$$

where Kf and n are Freundlich coefficients. Kf and $1/n$ are correlated to the sorption capacity and intensity of the system.

As shown in Figure 12, the RB19D adsorption exhibited the Langmuir isotherm of monolayer adsorption. It was demonstrated that the maximum adsorption capacity was 6.5 milligrams of dye per milligram of adsorbent. They were thought to adsorb at a small number of specific locations inside the calcium phosphate. On the other hand, DR1D exhibited Freundlich isotherms (Figure 12) of having more than one layer. The DR1D was shown to have a maximum adsorption capacity of 5.8 milligrams of dye per milligram of adsorbent.

4.6. COD, BOD, and TSS Analysis. The total COD measured before treatment was 2570, 2500, and 2370 ppm in the RB109D, DR1D, and BTSC effluents, respectively (Table 6). Those values confirmed that organic and inorganic materials are hazardous to health, so the wastewater must be treated. After treatment with CNP adsorbent, the COD values of the three categories of samples decreased by 82%, 87%, and 70%, respectively (Figure 13). When administered a synthetic coagulant, as described by [93] and [94], we achieved a removal rate of 55.2%, which is better than the current treatment. Besides environmental hazards, azo dyes are very toxic because of the reduction and breakdown of the azo bonds to produce toxic aromatic amines. Aromatic amines oxidize because of the direct oxidation of the azo bond, linking them to very reactive electrophilic diazonium salts and azo dyes [95]. Since each pathway could be compound-specific, azo toxicity is most likely brought on by several mechanisms. The azo dyes' altered intermediates have been shown to be very poisonous and mutagenic.

The findings before treatment show that the BOD values for RB109D, DR1D, and BTSC were 6200 ppm, 4515 ppm, and 4460 mg/L, respectively (Table 6). After treatment, the BOD values for RB109D, DR1D, and BTSC were 89, 90, and 89%, respectively (Figure 13). Compared to the current study, others reported reducing the BOD of textile effluent to 51.4% [94] and 82% [96] using synthetic coagulant. So, the current treatment is effective.

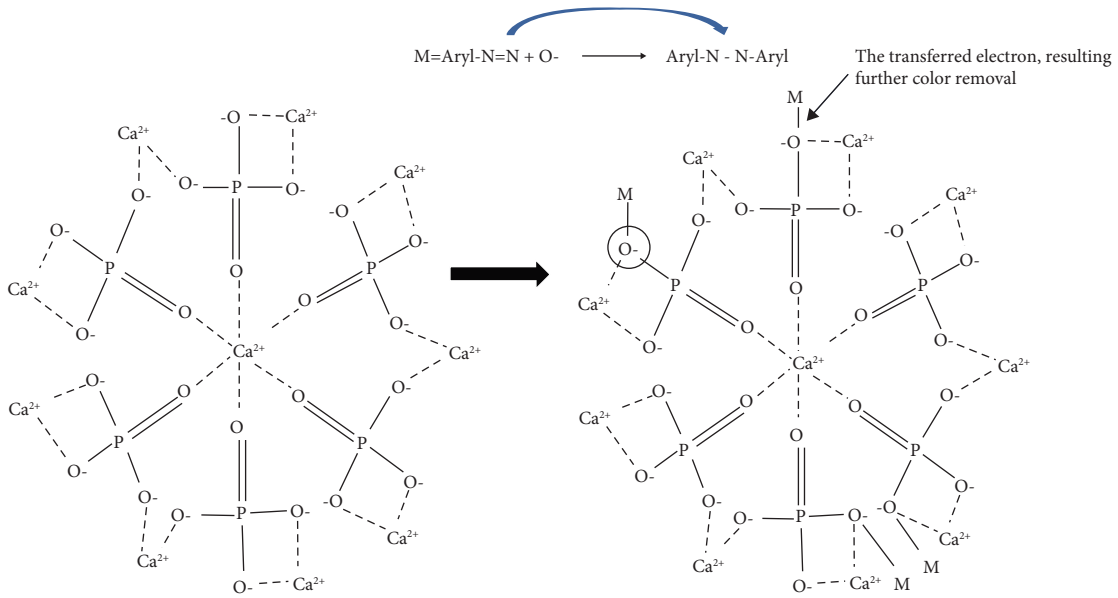

Figure 8: Schematic sketch of possible interaction between azo-nitrogen and hydroxyl groups in hydroxyapatite.

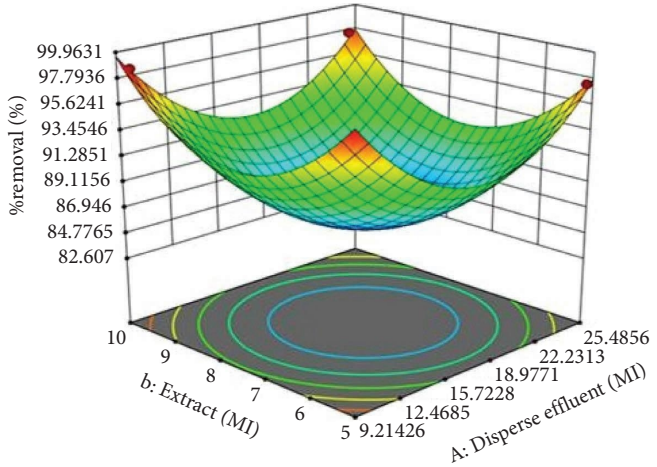

Figure 9: Interaction effect of the extract and the DR1D effluent concentrations on % removal of the color.

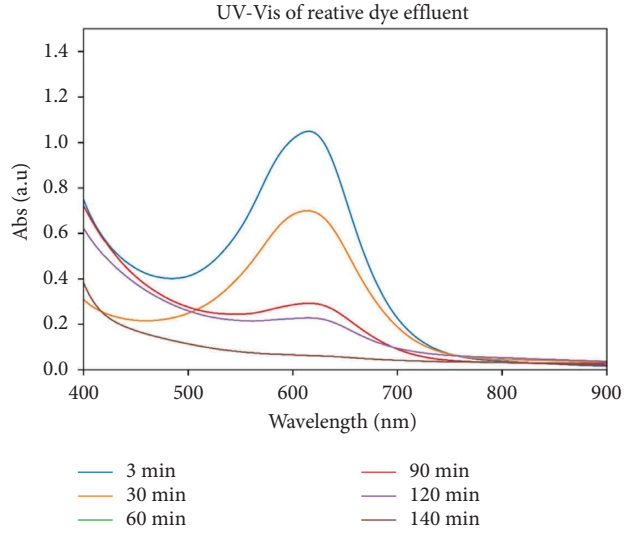

Figure 10: Adsorption spectra of RB19D effluent samples of variable contact time.

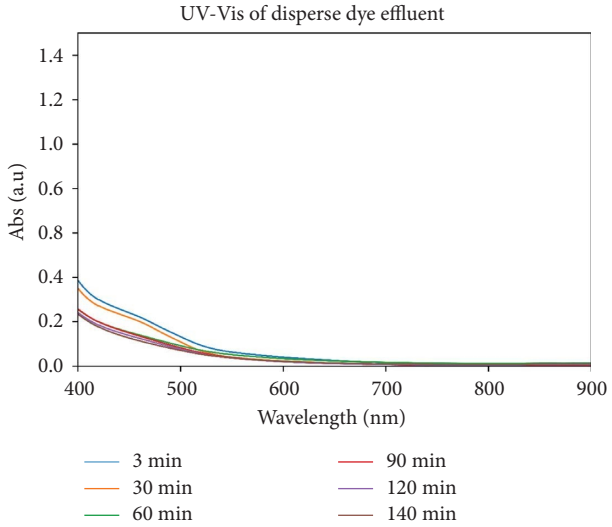

Figure 11: Adsorption spectra of DR1D effluent samples of variable contact time.

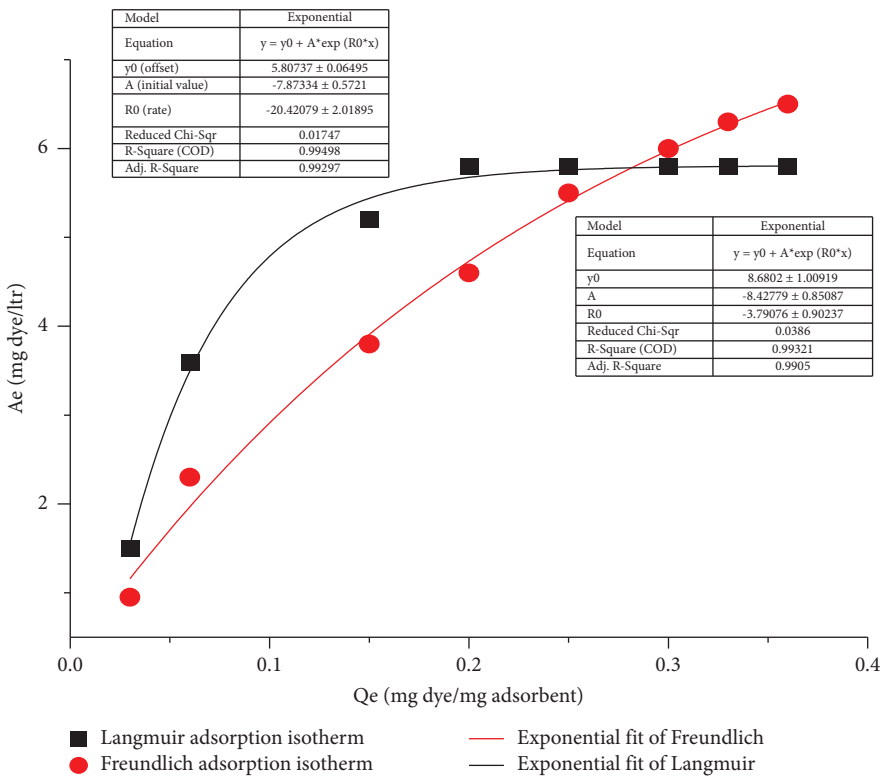

Figure 12: Raw data and exponentially fitted adsorption isotherm plots of Freundlich (DR1D dye) and Langmuir (RB19D dye), where x = Qe (mg dye/mg adsorbent) and y = Ae (mg dye/ltr of aqueous).

Table 6: Oxygen demand, turbidity, and total solid analysis (treatment time = 90 min).

Dye parameters	Untreated RB19D	Treated RB19D	Untreated DR1D	Treated DR1D	Untreated BTSC DR1D	Treated BTSC DR1D
COD, ppm	2,570	460	2,500	328	2350	695
BOD, ppm	1,840	208	1,800	184	1900	210
TSS, mg/L	6,200	1,780	4,515	1,250	4,460	2,004

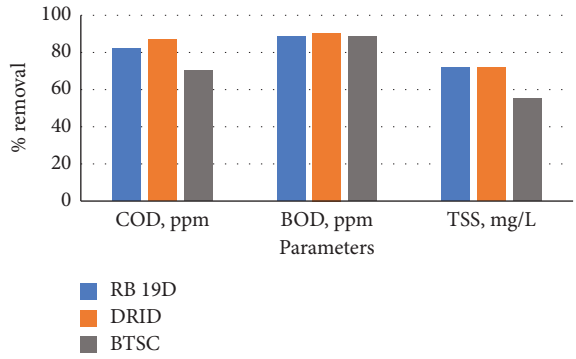

Figure 13: Percentage removal of COD, BOD, and TSS from effluents after treatment with biocomponet adsorbent.

Before the treatment, TSS for RB109D, DR1D, and BTSC were 6200, 4515, and 4460 mg/L, respectively (Table 6). The result shows a large amount of pollution is caused due to the textile wastewater which is also determined by other researchers [97]. After treatment, the TSS value of the treated samples exhibited remarkable results having TSS percentage removal of 82%, 89%, and 71%, respectively (Figure 13).

5. Conclusion

Animal bone wastes are being used as a substitute adsorbent in the current study to treat textiles dye effluent. The CNP biocomponent precipitate, which included calcium and phosphate ions, was used to treat RB109D and DR1D effluents. The molecular composition of the extracted adsorbent was analyzed by FTIR, showing spectral peaks of calcium and phosphate chelates. The CNP biocomponent from animal bones can adsorb color from aqueous RB109D and DR1D effluents in one hour. UV-Vis analyses were made to analyze how fast the color removal and other residues took place. The chemistry of discoloration was caused by the reductive breaking of azo bonds (-N=N-) with reductive oxygen. The adsorption pattern shows the Langmuir isotherm in the case of RB109D effluent. On the other hand, DR1D exhibited Freundlich isotherms. The average color removal of 92.68% and 95.66% was achieved for RB109D and DR1D, respectively. The extracted adsorbent and effluent water concentration showed an upward parabolic effect on the percentage of color removal from the DR1D effluent, whereas in the case of RB109D, both the extracted adsorbent and effluent water concentration showed a negative correlation with the percentage of color removal. Therefore, the adsorbent was shown to be significant in removing the coloring matter from both dye types.

For industrial uses, our team has been focusing on the chemical-free extraction of the CNP biocomponent. As a future work, the reuse of the treated water, sludge for composite application, and regeneration of the calcium phosphate after treatment needs experimentation.

Data Availability

The experimental data used to support the findings of this study are included within the article.

Conflicts of Interest

The authors declare that they have no conflicts of interest.

Authors' Contributions

Natinael Kokeb and Dr. Tamrat Tesfaye handled conceptualization and experimental design. Natinael Kokeb and Tinsaye Asfaw were in charge of the literature review. Gemeda Gebino and Dr. Shalemu Sharew conducted the experiment.

References

[1] F. M. Drumond Chequer, G. A. R. de Oliveira, E. R. Anastacio Ferraz, J. Carvalho, M. V. Boldrin Zanoni, and D. P. de Oliveir, "Textile dyes: dyeing process and environmental impact," in *Eco-Friendly Textile Dyeing and Finishing*, IntechOpen, London, UK, 2013.

[2] P. Senthil Kumar and E. Gunasundari, "Sustainable wet processing—an alternative source for detoxifying supply chain in textiles," *Detox Fashion: Sustainable Chemistry and Wet Processing*, Springer, Berlin, Germany, 2018.

[3] X. Wang, J. Jiang, and W. Gao, "Reviewing textile wastewater produced by industries: characteristics, environmental impacts, and treatment strategies," *Water Science and Technology*, vol. 85, no. 7, pp. 2076–2096, 2022.

[4] M. W. Rundassa, D. K. Azene, and E. Berhan, "Comparative advantage of Ethiopian textile and apparel industry," *Research Journal of Textile and Apparel*, vol. 23, no. 3, pp. 244–256, 2019.

[5] G. Mustafa, M. Tariq Zahid, S. Ali, S. Zaghum Abbas, and M. Rafatullah, "Biodegradation and discoloration of disperse blue-284 textile dye by Klebsiella pneumoniae GM-04 bacterial isolate," *Journal of King Saud University Science*, vol. 33, no. 4, Article ID 101442, 2021.

[6] A. O. Basilio, L. Dohler, M. Servin, C. A. K. Gouvea, R. R. Ribeiro, and P. Peralta-Zamora, "Degradation of reactive dyes by thermally activated persulfate and reuse of treated textile dye-bath," *Journal of the Brazilian Chemical Society*, vol. 32, no. 9, 2021.

[7] F. Feng, Z. Xu, X. Li, W. You, and Y. Zhen, "Advanced treatment of dyeing wastewater towards reuse by the combined Fenton oxidation and membrane bioreactor process," *Journal of Environmental Sciences*, vol. 22, no. 11, pp. 1657–1665, 2010.

[8] X. L. Zou, "Combination of ozonation, activated carbon, and biological aerated filter for advanced treatment of dyeing wastewater for reuse," *Environmental Science and Pollution Research*, vol. 22, no. 11, pp. 8174–8181, 2015.

[9] S. Madhav, A. Ahamad, P. Singh, and P. K. Mishra, "A review of textile industry: wet processing, environmental impacts, and effluent treatment methods," *Environmental Quality Management*, vol. 27, no. 3, pp. 31–41, 2018.

[10] T. Robinson, G. McMullan, R. Marchant, and P. Nigam, "Remediation of dyes in textile effluent: a critical review on current treatment technologies with a proposed alternative," *Bioresource Technology*, vol. 77, no. 3, pp. 247–255, 2001.

[11] P. Sasirekha, S. Shankar Krishna, S. Vembukumar, and L. Vignesh, "Ecofriendly decolorisation of textile waste water using natural coagulants," *Asian Journal of Engineering and Applied Technology*, vol. 8, no. 2, pp. 41–44, 2019.

[12] B. T. Wagaye and G. A. Walle, "Overview of Ethiopian textile industry," *Journal of Textiles and Polymers*, vol. 6, no. 2, 2018.

[13] A. H. Mahvi, M. Ghanbarian, S. Nasseri, and A. Khairi, "Mineralization and discoloration of textile wastewater by TiO2 nanoparticles," *Desalination*, vol. 239, no. 1–3, pp. 309–316, 2009.

[14] S. Natarajan, H. C. Bajaj, and R. J. Tayade, "Recent advances based on the synergetic effect of adsorption for removal of dyes from waste water using photocatalytic process," *Journal of Environmental Sciences*, vol. 65, pp. 201–222, 2018.

[15] F. Al-Momani, E. Touraud, J. R. Degorce-Dumas, J. Roussy, and O. Thomas, "Biodegradability enhancement of textile dyes and textile wastewater by VUV photolysis," *Journal of Photochemistry and Photobiology A: Chemistry*, vol. 153, no. 1–3, pp. 191–197, 2002.

[16] J. M. Aquino, G. F. Pereira, R. C. Rocha-Filho, N. Bocchi, and S. R. Biaggio, "Combined coagulation and electrochemical process to treat and detoxify a real textile effluent," *Water, Air, & Soil Pollution*, vol. 227, no. 8, 2016.

[17] S. Bouznif and M. Bali, "Coupling of the coagulation/flocculation and the anodic oxidation processes for the treatment of textile wastewater," *Journal of Water Supply: Research & Technology-Aqua*, vol. 70, no. 4, pp. 587–599, 2021.

[18] N. H. Torres, B. S. Souza, L. F. R. Ferreira, A. S. Lima, G. N. dos Santos, and E. B. Cavalcanti, "Real textile effluents treatment using coagulation/flocculation followed by electrochemical oxidation process and ecotoxicological assessment," *Chemosphere*, vol. 236, Article ID 124309, 2019.

[19] A. Geethakarthi, "Application of sustainable and low-cost sludge-based adsorbents for textile dye degradation," *Advances in Textile Waste Water Treatments*, Springer, Berlin, Germany, 2021.

[20] V. Parameswaran, E. R. Nagarajan, and A. Murugan, "Treatment of textile effluents by ion-exchange polymeric materials," *International Journal of ChemTech Research*, vol. 6, 2014.

[21] D. Suteu and S. Coseri, "Applications of polymeric materials as adsorbents for dyes removal from aqueous medium," *Polymer Science: Research Advances, Practical Applications and Educational Aspects*, 2016.

[22] M. F Zawrah, M. I El-Gammal, M. Salem, M. A El-Sonbati, and M. Ahmed, "Synthesis and characterization of activated carbon from rice husk for wastewater treatment," *Journal of Environmental Sciences. Mansoura University*, vol. 49, no. 4, pp. 106–112, 2020.

[23] A. B. Lamido, "Efficiency of activated carbon produced from rice husk in water treatment," *International Journal for Research in Applied Science and Engineering Technology*, vol. 8, no. 6, pp. 439–443, 2020.

[24] G. C. Pei, R. M. Ghazi, N. R. Nik Yusoff, M. Z. Mohd Alias, and M. Jani, "Adsorption of COD in wastewater by activated carbon from rice husk," in *Proceedings of the IOP Conference Series: Earth and Environmental Science*, vol. 596, no. 1, Malaysia, September 2020.

[25] M. I. Aydin, B. Yuzer, A. Ongen, H. E. Okten, and H. Selcuk, "Comparison of ozonation and coagulation decolorization methods in real textile wastewater," *Desalination and Water Treatment*, vol. 103, pp. 5–64, 2018.

[26] J. Perkowski, L. Kos, and S. Ledakowicz, "Application of ozone in textile wastewater treatment," *Ozone: Science & Engineering*, vol. 18, no. 1, pp. 73–85, 1996.

[27] S. S. Hutagalung, I. Muchlis, and K. Khotimah, "Textile wastewater treatment using advanced oxidation process (AOP)," in *Proceedings of the IOP Conference Series: Materials Science and Engineering*, vol. 722, no. 1, Yogyakarta, Indonesia, October 2020.

[28] Y. Zhang, K. Shaad, D. Vollmer, and C. Ma, "Treatment of textile wastewater using advanced oxidation processes—a critical review," *Water*, vol. 13, no. 24, p. 3515, 2021.

[29] R. Khan, P. Bhawana, and M. H. Fulekar, "Microbial decolorization and degradation of synthetic dyes: a review," *Reviews in Environmental Science and Biotechnology*, vol. 12, no. 1, pp. 75–97, 2013.

[30] W. P. Mon, P. Jantaharn, S. Boonlue, S. McCloskey, S. Kanokmedhakul, and W. Mongkolthanaruk, "Enzymatic degradation of Azo bonds and other functional groups on commercial silk dyes by streptomyces coelicoflavus CS-29," *Environment and Natural Resources Journal*, vol. 20, no. 1, pp. 1–10, 2022.

[31] R. G. Saratale, G. D. Saratale, J. S. Chang, and S. P. Govindwar, "Bacterial decolorization and degradation of azo dyes: a review," *Journal of the Taiwan Institute of Chemical Engineers*, vol. 42, no. 1, pp. 138–157, 2011.

[32] R. L. Singh, P. K. Singh, and R. P. Singh, "Enzymatic decolorization and degradation of azo dyes-a review," *International Biodeterioration & Biodegradation*, vol. 104, pp. 21–31, 2015.

[33] J. B. Schallemberger, N. Libardi, B. L. S. K. Dalari, M. B. Chaves, and M. E. Nagel Hassemer, "Textile azo dyes discolouration using spent mushroom substrate: enzymatic degradation and adsorption mechanisms," *Environmental Technology*, vol. 44, no. 9, pp. 1265–1286, 2021.

[34] M. Gebrezgiher and Z. Kiflie, "Utilization of cactus peel as biosorbent for the removal of reactive dyes from textile dye effluents," *Journal of Environmental and Public Health*, vol. 2020, Article ID 5383842, 10 pages, 2020.

[35] H. N. J. Hoong and N. Ismail, "Removal of dye in wastewater by adsorption-coagulation combined system with Hibiscus sabdariffa as the coagulant," *MATEC Web of Conferences*, vol. 152, Article ID 01008, 2018.

[36] A. T. Mansour, A. E. Alprol, K. M. Abualnaja, H. S. El-Beltagi, K. M. A. Ramadan, and M. Ashour, "Dried Brown seaweed's phytoremediation potential for methylene blue dye removal from aquatic environments," *Polymers*, vol. 14, no. 7, p. 1375, 2022.

[37] R. A. Moura, A. A. Seolatto, M. E. de Oliveira Ferreira, and F. F. Freitas, "The adsorption study of Royal Blue Tiafix and Black Tiassolan dyes using bone char as adsorbent," *Adsorption Science and Technology*, vol. 36, no. 3–4, pp. 1178–1198, 2018.

[38] Y. Chen, L. Feng, H. Li, Y. Wang, G. Chen, and Q. Zhang, "Biodegradation and detoxification of Direct Black G textile dye by a newly isolated thermophilic microflora," *Bioresource Technology*, vol. 250, pp. 650–657, 2018.

[39] M. Manivannan, D. Reetha, and P. Ganesh, "Decolourization of textile azo dyes by using bacteria isolated from textile dye effluent," *Journal of Ecobiotechnology*, vol. 3, no. 8, 2011.

[40] P. Saranraj, V. Sumathi, D. Reetha, and D. Stella, "Decolourization and degradation of dirct azo dyes and biodegradation of textile dye effluent by using bacteria isolated from textile dye effluent," *Journal of Ecobiotechnology*, vol. 2, 2010.

[41] A. Dabassa, "Evaluation of home slaughtered meat quality used for human consumption at household and food seller house in Jimma," *Journal of Medical Sciences*, vol. 13, no. 8, pp. 779–784, 2013.

[42] S. Seleshe, C. Jo, and M. Lee, "Meat consumption culture in Ethiopia," *Korean Journal for Food Science of Animal Resources*, vol. 34, no. 1, pp. 7–13, 2014.

[43] P. Rozi, P. Maimaiti, A. Abuduwaili, A. Wali, A. Yili, and H. A. Aisa, "Isolation and evaluation of bioactive protein and peptide from domestic animals' bone marrow," *Molecules*, vol. 23, no. 7, p. 1673, 2018.

[44] J. K. Abifarin, D. O. Obada, E. T. Dauda, and D. Dodoo-Arhin, "Experimental data on the characterization of hydroxyapatite synthesized from biowastes," *Data in Brief*, vol. 26, Article ID 104485, 2019.

[45] A. T. Hexter, C. Pendegrass, F. Haddad, and G. Blunn, "Demineralized bone matrix to augment tendon- bone healing: a systematic review," *Orthopaedic Journal of Sports Medicine*, vol. 5, no. 10, Article ID 232596711773451, 2017.

[46] P. Dericquebourg, A. Person, L. Ségalen, M. Pickford, B. Senut, and N. Fagel, "Bone diagenesis and origin of calcium phosphate nodules from a hominid site in the Lukeino Formation (Tugen Hills, Kenya)," *Palaeogeography, Palaeoclimatology, Palaeoecology*, vol. 536, Article ID 109377, 2019.

[47] F. Pahlevanzadeh, H. R. Bakhsheshi-Rad, and E. Hamzah, "In-vitro biocompatibility, bioactivity, and mechanical strength of PMMA-PCL polymer containing fluorapatite and graphene oxide bone cements," *Journal of the Mechanical Behavior of Biomedical Materials*, vol. 82, pp. 257–267, 2018.

[48] G. Falini, M. L. Basile, S. Gandolfi et al., "Natural calcium phosphates from circular economy as adsorbent phases for the remediation of textile industry waste-waters," *Ceramics International*, vol. 49, no. 1, pp. 243–252, 2023.

[49] Y. A. B. Neolaka, Y. Lawa, J. Naat et al., "Adsorption of methyl red from aqueous solution using Bali cow bones (Bos javanicus domesticus) hydrochar powder," *Results in Engineering*, vol. 17, Article ID 100824, 2023.

[50] A. I. Adeogun, E. A. Ofudje, M. A. Idowu, S. O. Kareem, S. Vahidhabanu, and B. R. Babu, "Biowaste-Derived hydroxyapatite for effective removal of reactive yellow 4 dye: equilibrium, kinetic, and thermodynamic studies," *ACS Omega*, vol. 3, no. 2, pp. 1991–2000, 2018.

[51] M. Amin, G. A. Al Bazedi, and E. Abadir, "Treatment of blue HB reactive dyes in textile wastewater using bio-waste based hydroxyapatite," *Egyptian Journal of Chemistry*, vol. 0, no. 0, pp. 0–2, 2022.

[52] E. A. Ofudje, I. A. Adeogun, M. A. Idowu, S. O. Kareem, and N. A. Ndukwe, "Simultaneous removals of cadmium (II) ions and reactive yellow 4 dye from aqueous solution by bone meal-derived apatite: kinetics, equilibrium and thermodynamic evaluations," *Journal of Analytical Science and Technology*, vol. 11, no. 1, 2020.

[53] P. Sirajudheen, P. Karthikeyan, S. Vigneshwaran, and S. Meenakshi, "Complex interior and surface modified alginate reinforced reduced graphene oxide-hydroxyapatite hybrids: removal of toxic azo dyes from the aqueous solution," *International Journal of Biological Macromolecules*, vol. 175, pp. 361–371, 2021.

[54] A. Guesmi, M. M. Cherif, O. Baaloudj et al., "Disinfection of corona and myriad viruses in water by non-thermal plasma: a review," *Environmental Science and Pollution Research*, vol. 29, no. 37, pp. 55321–55335, 2022.

[55] K. N. Pandiyaraj, D. Vasu, R. Ghobeira et al., "Dye wastewater degradation by the synergetic effect of an atmospheric pressure plasma treatment and the photocatalytic activity of plasma-functionalized Cu–TiO2 nanoparticles," *Journal of Hazardous Materials*, vol. 405, Article ID 124264, 2021.

[56] M. M. Rashid, M. Chowdhury, and M. R. Talukder, "Textile wastewater treatment by underwater parallel-multi-tube air discharge plasma jet," *Journal of Environmental Chemical Engineering*, vol. 8, no. 6, Article ID 104504, 2020.

[57] D. Vasu, K. Navaneetha Pandiyaraj, P. V. A. Padmanabhan, M. Pichumani, R. R. Deshmukh, and S. K. Jaganathan, "Degradation of simulated Direct Orange-S (DO-S) textile effluent using nonthermal atmospheric pressure plasma jet," *Environmental Geochemistry and Health*, vol. 43, no. 2, pp. 649–662, 2021.

[58] M. Laktionov, L. Nová, and O. V. Rud, "Water desalination using polyelectrolyte hydrogel: gibbs ensemble modeling," *Gels*, vol. 8, no. 10, p. 656, 2022.

[59] H. Mittal, S. S. Ray, and M. Okamoto, "Recent progress on the design and applications of polysaccharide-based graft copolymer hydrogels as adsorbents for wastewater purification," *Macromolecular Materials and Engineering*, vol. 301, no. 5, pp. 496–522, 2016.

[60] O. V. Rud, A. D. Kazakov, L. Nova, and F. Uhlik, "Polyelectrolyte hydrogels as draw agents for desalination of solutions with multivalent ions," *Macromolecules*, vol. 55, no. 5, pp. 1763–1770, 2022.

[61] O. Baaloudj, H. Kenfoud, A. K. Badawi et al., "Bismuth sillenite crystals as recent photocatalysts for water treatment and energy generation: a critical review," *Catalysts*, vol. 12, no. 5, p. 500, 2022.

[62] H. R. Dihom, M. M. Al-Shaibani, R. M. S. Radin Mohamed, A. A. Al-Gheethi, A. Sharma, and M. H. B. Khamidun, "Photocatalytic degradation of disperse azo dyes in textile wastewater using green zinc oxide nanoparticles synthesized in plant extract: a critical review," *Journal of Water Process Engineering*, vol. 47, Article ID 102705, 2022.

[63] A. Kane, A. A. Assadi, A. El Jery et al., "Advanced photocatalytic treatment of wastewater using immobilized titanium dioxide as a photocatalyst in a pilot-scale reactor: process intensification," *Materials*, vol. 15, no. 13, p. 4547, 2022.

[64] K. Krawczyk, S. Wacławek, E. Kudlek et al., "Uv-catalyzed persulfate oxidation of an anthraquinone based dye," *Catalysts*, vol. 10, no. 4, p. 456, 2020.

[65] S. P. F. Bernal, M. M. A. Lira, J. Jean-Baptiste et al., "Biotechnological potential of microorganisms from textile effluent: isolation, enzymatic activity and dye discoloration," *Anais da Academia Brasileira de Ciencias*, vol. 93, no. 4, 2021.

[66] M. J. M-Ridha, S. I. Hussein, Z. T. Alismaeel, M. A. Atiya, and G. M. Aziz, "Biodegradation of reactive dyes by some bacteria using response surface methodology as an optimization technique," *Alexandria Engineering Journal*, vol. 59, no. 5, pp. 3551–3563, 2020.

[67] Y. Qu, S. Shi, F. Ma, and B. Yan, "Decolorization of Reactive Dark Blue K-R by the synergism of fungus and bacterium using response surface methodology," *Bioresource Technology*, vol. 101, no. 21, pp. 8016–8023, 2010.

[68] V. S. Gshalaev and A. C. Demirchan, *Hydroxyapatite: Synthesis, Properties and Applications*, Nova Science Publishers, Hauppauge, NY, USA, 2013.

[69] A. R. Toibah, F. Misran, Z. Mustafa, A. Shaaban, and S. R. Shamsuri, "Calcium phosphate from waste animal bones: phase identification analysis," *Journal of Advanced Manufacturing Technology*, vol. 12, 2018.

[70] A. C. L. de Assis, L. P. Alves, J. P. T. Malheiro et al., "Opuntia ficus-indica L. Miller (palma forrageira) as an alternative source of cellulose for production of pharmaceutical dosage forms and biomaterials: extraction and characterization," *Polymers*, vol. 11, no. 7, p. 1124, 2019.

[71] C. S. Seo, J. H. Kim, and H. K. Shin, "Optimization of the extraction process for the seven bioactive compounds in Yukmijihwang-tang, an herbal formula, using response

surface methodology," *Pharmacognosy Magazine*, vol. 10, no. 39, p. 606, 2014.

[72] D. A. Yaseen and M. Scholz, "Treatment of synthetic textile wastewater containing dye mixtures with microcosms," *Environmental Science and Pollution Research*, vol. 25, no. 2, pp. 1980–1997, 2018.

[73] T. Rashid, D. Iqbal, A. Hazafa, S. Hussain, F. Sher, and F. Sher, "Formulation of zeolite supported nano-metallic catalyst and applications in textile effluent treatment," *Journal of Environmental Chemical Engineering*, vol. 8, no. 4, Article ID 104023, 2020.

[74] M. A. Al-Ghouti and D. A. Da'ana, "Guidelines for the use and interpretation of adsorption isotherm models: a review," *Journal of Hazardous Materials*, vol. 393, Article ID 122383, 2020.

[75] S. V. Dorozhkin, "Surface reactions of apatite dissolution," *Journal of Colloid and Interface Science*, vol. 191, no. 2, pp. 489–497, 1997.

[76] M. W. Guidry and F. T. Mackenzie, "Experimental study of igneous and sedimentary apatite dissolution: control of pH, distance from equilibrium, and temperature on dissolution rates," *Geochimica et Cosmochimica Acta*, vol. 67, no. 16, pp. 2949–2963, 2003.

[77] J. Oliva, J. Cama, J. L. Cortina, C. Ayora, and J. de Pablo, "Biogenic hydroxyapatite (Apatite II^{TM}) dissolution kinetics and metal removal from acid mine drainage," *Journal of Hazardous Materials*, vol. 213-214, pp. 7–18, 2012.

[78] C. E. Calmanovici, B. Gilot, and C. Laguerie, "Mechanism and kinetics for the dissolution of apatitic materials in acid solutions," *Brazilian Journal of Chemical Engineering*, vol. 14, no. 2, pp. 95–102, 1997.

[79] P. Basak, P. Pahari, P. Das, N. Das, S. K. Samanta, and S. Roy, "Synthesis and characterisation of gelatin-PVA/hydroxyapetite(HAP) composite for medical applications," in *Proceedings of the IOP Conference Series: Materials Science and Engineering*, vol. 410, no. 1, Odisha, India, September 2018.

[80] L. D. Mkukuma, J. M. S. Skakle, I. R. Gibson, C. T. Imrie, R. M. Aspden, and D. W. L. Hukins, "Effect of the proportion of organic material in bone on thermal decomposition of bone mineral: an investigation of a variety of bones from different species using thermogravimetric analysis coupled to mass spectrometry, high-temperature X-ray diffraction, and fourier transform infrared spectroscopy," *Calcified Tissue International*, vol. 75, no. 4, pp. 321–328, 2004.

[81] K. C. Vinoth Kumar, T. Jani Subha, K. G. Ahila et al., "Spectral characterization of hydroxyapatite extracted from Black Sumatra and Fighting cock bone samples: a comparative analysis," *Saudi Journal of Biological Sciences*, vol. 28, no. 1, pp. 840–846, 2021.

[82] R. Venkataraghavan, R. Thiruchelvi, and D. Sharmila, "Statistical optimization of textile dye effluent adsorption by Gracilaria edulis using Plackett-Burman design and response surface methodology," *Heliyon*, vol. 6, no. 10, 2020.

[83] C. Smaranda, D. Bulgariu, and M. Gavrilescu, "An investigation of the sorption of Acid Orange 7 from aqueous solution onto soil," *Environmental Engineering and Management Journal*, vol. 8, no. 6, pp. 1391–1402, 2009.

[84] S. Pai, S. M Kini, R. Selvaraj, and A. Pugazhendhi, "A review on the synthesis of hydroxyapatite, its composites and adsorptive removal of pollutants from wastewater," *Journal of Water Process Engineering*, vol. 38, 2020.

[85] W. Lemlikchi, P. Sharrock, M. O. Mecherri, M. Fiallo, and A. Nzihou, "Reaction of calcium phosphate with textile dyes for purification of wastewaters," *Desalination and Water Treatment*, vol. 52, no. 7–9, pp. 1669–1673, 2014.

[86] R. P. F. Melo, S. K. S. Carmo, E. L. B. Barros, A. G. Câmara, S. K. S. Nunes, and E. L. Barros Neto, "Removal of Disperse Blue 56 from synthetic textile effluent using ionic flocculation," *Water Science and Technology*, vol. 83, no. 11, pp. 2714–2723, 2021.

[87] S. S. Ashraf, M. A. Rauf, and S. Alhadrami, "Degradation of Methyl Red using Fenton's reagent and the effect of various salts," *Dyes and Pigments*, vol. 69, no. 1–2, pp. 74–78, 2006.

[88] M. el Haddad, R. Slimani, R. Mamouni, S. ElAntri, and S. Lazar, "Removal of two textile dyes from aqueous solutions onto calcined bones," *Journal of the Association of Arab Universities for Basic and Applied Sciences*, vol. 14, no. 1, pp. 51–59, 2013.

[89] N. Bougdour, R. Tiskatine, I. Bakas, and A. Assabbane, "Textile wastewater treatment by peroxydisulfate/Fe(II)/UV: operating cost evaluation and phytotoxicity studies," *Chemistry Africa*, vol. 3, no. 1, pp. 153–160, 2020.

[90] F. Ali, N. Ali, I. Bibi et al., "Adsorption isotherm, kinetics and thermodynamic of acid blue and basic blue dyes onto activated charcoal," *Case Studies in Chemical and Environmental Engineering*, vol. 2, Article ID 100040, 2020.

[91] V. K. Verma and A. K. Mishra, "Kinetic and isotherm modeling of adsorption of dyes onto rice husk carbon," *Global Nest Journal*, vol. 12, no. 2, 2010.

[92] Z. A. Hammood, T. F. Chyad, and R. Al-Saedi, "Adsorption performance of dyes over zeolite for textile wastewater treatment," *Ecological Chemistry and Engineering S*, vol. 28, no. 3, pp. 329–337, 2021.

[93] E. Bazrafshan, M. R. Alipour, and A. H. Mahvi, "Textile wastewater treatment by application of combined chemical coagulation, electrocoagulation, and adsorption processes," *Desalination and Water Treatment*, vol. 57, no. 20, pp. 9203–9215, 2016.

[94] H. Patel and R. T. Vashi, "Treatment of textile wastewater by adsorption and coagulation," *E-Journal of Chemistry*, vol. 7, no. 4, pp. 1468–1476, 2010.

[95] L. Wojnárovits, T. Pálfi, and E. Takács, "Kinetics and mechanism of azo dye destruction in advanced oxidation processes," *Radiation Physics and Chemistry*, vol. 76, no. 8–9, pp. 1497–1501, 2007.

[96] M. R. Islam and M. G. Mostafa, "Characterization of textile dyeing effluent and its treatment using polyaluminum chloride," *Applied Water Science*, vol. 10, no. 5, 2020.

[97] A. Munnaf, M. Islam, T. Tusher, M. Kabir, and M. Molla, "Investigation of water quality parameters discharged from textile dyeing industries," *Journal of Environmental Science and Natural Resources*, vol. 7, no. 1, pp. 257–263, 2015.